New Elemental Abundances for V1974 Cygni

K.M. Vanlandingham
Columbia University, Department of Astronomy, New York, NY 10027
kmv14@columbia.edu

G.J. Schwarz
Steward Observatory, University of Arizona, Tucson, AZ 85721
gschwarz@as.arizona.edu

S.N. Shore
Dipartimento di Fisica "Enrico Fermi", Università di Pisa, largo Pontecorvo 3, Pisa 56127, Italy
shore@df.unipi.it

S. Starrfield
Department of Physics & Astronomy, Arizona State University, Tempe, AZ 85287-1504
sumner.starrfield@asu.edu
and

R.M. Wagner
Steward Observatory, University of Arizona, Tucson, AZ 85721
rmw@as.arizona.edu

ABSTRACT

We present a new analysis of existing optical and ultraviolet spectra of the ONeMg nova V1974 Cygni 1992. Using these data and the photoionization code Cloudy, we have determined the physical parameters and elemental abundances for this nova. Many of the previous studies of this nova have made use of incorrect analyses and hence a new study was required. Our results show that the ejecta are enhanced, relative to solar, in helium, nitrogen, oxygen, neon, magnesium and iron. Carbon was found to be subsolar. We find an ejected mass of $\sim 2\times10^{-4}M_{\odot}$. Our model results fit well with observations taken at IR, radio, sub-millimeter and X-ray wavelengths.

Subject headings: novae, binary stars,stars:individual (V1974 Cyg), stars:abundances

1. Introduction

Novae explosions are the result of a thermonuclear runaway (TNR) occurring on the surface of a white dwarf (WD) in a close binary system. Material is transferred from the secondary star, a late-type main-sequence star, through the inner Lagrangian point to an accretion disk and then onto the WD. Once enough material is accreted nuclear fusion begins in the surface layers of the WD. Since the WD is degenerate, this leads to a TNR that then results in the ejection of the accreted material. Analysis of the ejecta provides information about the physics of the nova process and the WDs on which they take place.

V1974 Cygni 1992 (hereafter Cyg 92) was discovered on 1992 February 19 by Collins (1992) (taken to be t_0 in this paper). At that time it was the brightest nova since V1500 Cygni and hence was one of the most extensively observed novae in history with observations spanning the entire spectral range from gamma-rays to radio. Ultraviolet (UV) observations made with the International Ultraviolet Explorer satellite (IUE) show that Cyg 92 was a "neon" nova - one that takes place on an ONeMg WD.

Three detailed abundance analyses have been carried out for Cyg 92: Austin et al. (1996, hereafter A96), Hayward et al. (1996) & Moro-Martín et al. (2001). Unfortunately these analyses were based on data that was dereddened incorrectly. In the initial analysis by A96 the reddening correction was applied in the wrong direction for the optical spectra. In other words, the optical spectra were *reddened* rather than *dereddened*. The UV spectra were dereddened correctly, however since the analyses relied on the flux ratios relative to Hβ the UV ratios were ultimately affected by this mistake. Hence a new analysis is required. Using optical and UV data we have determined physical parameters and elemental abundances for Cyg 92. While we have used the same photoionization code as A96 and Moro-Martín, we have developed a two-component model to simulate the inhomogeniety of the nova shell which is more physically accurate than these other analyses. Hayward et al. also used a multi-component model in their work however we have included significantly more data in our analysis than they did. We have compared our results with X-ray, infrared (IR), sub-millimeter, and radio data in the literature and find them consistent.

In Section 2 we briefly describe the observations used in our analysis. Section 3 reviews the reddening to the nova. An overview of our analysis technique is given in Section 4. Section 5 contains a detailed description of our model results and these results are compared to others in the literature in Section 6. Our conclusions and summary are given in Section 7.

2. Observations

The UV data were obtained with IUE. Low-dispersion large-aperture data were taken with both the Short Wavelength Primary (SWP: 1200-2000Å) and the Long Wavelength Primary (LWP: 2000-3400Å) cameras (resolution 7Å). The data were reduced at the Goddard Space Flight Center (GSFC) Regional Data Analysis Facility (RDAF) using the NEWSIPS IUE soft-

ware. The optical data were taken with the Perkins 1.8-m telescope at Lowell Observatory using the Ohio State University Boller & Chivens spectrograph (resolution 6Å, wavelength range 3200-8450Å). For a detailed description of the data and spectral evolution see A96. The data we are re-analyzing are the spectra taken roughly 300, 400 and 500 days after the outburst.

The optical spectra were not absolutely flux calibrated. In order to combine them with the UV data we had to scale the optical flux to match in the overlap region. This was done using the ratio of the He II lines at 1640Å and 4686Å. Osterbrock (1989) gives the theoretical ratio of these lines as 6.79. After correcting the spectra for reddening, we scaled the optical flux until the 1640/4686 ratio was equal to 6.79. The dereddened line fluxes are given in Table 1.

3. Reddening

A summary of reddening values used by other groups is given in Chochol et al. (1997, their Table 1). Published values for E(B-V) range from 0.17 to 0.42. For our analysis we have used two methods to determine the reddening. First we used the interstellar absorption feature at 2175Å. UV spectra taken with the Faint Object Spectrograph (FOS) on the Hubble Space Telescope (HST) on 1995 November 30 clearly show this feature. We have taken these data and applied several different reddening values using the extinction curve of Seaton (1979) and fit a line through the continuum. The spectra are shown in Figure 1. These data clearly favor higher reddening values with the best value being E(B-V)=0.36. For a second

Table 1: Dereddened Observed Line Fluxes[a]

Line ID	Day 300	Day 400	Day 500
N V 1240[b]	1616.5	7203.98	2284.19
O IV] 1402	526.25	117.49	26.92
N IV] 1486	865.56	202.34	49.46
C IV 1549	309.94	63.06	18.17
[Ne V] 1575	147.08	34.67	10.30
[Ne IV] 1602	403.26	96.16	21.71
He II 1640	233.66	56.89	18.29
O III] 1663	221.33	36.22	13.08
N III] 1750	379.42	64.90	17.98
C III] 1909	105.75	19.13	4.50
[Ne IV] 2424	66.69	64.70	-
Mg II 2798	221.02	59.73	5.9
[Ne V] 2976	100.11	57.96	5.1
[Ne V] 3346[c]	1627.95	612.36	372.28
[Ne V] 3426	4411.55	1833.24	1123.39
[Ne III] 3869	937.85	273.665	151.16
[Ne III] 3968	299.56	80.33	43.48
H I 4102	62.64	13.25	6.44
H I 4340	35.74	9.53	6.47
[O III] 4363	308.89	90.33	53.12
He II 4686	53.91	18.59	15.80
[Ne IV] 4721	199.00	62.34	31.63
H IV 4861	85.72	24.03	13.94
[O III] 4959	199.60	73.29	58.23
[O III] 5007	568.70	201.02	156.35
[N II] 5755	16.62	9.87	9.63
He I 5876	10.06	1.64	1.17
[Fe VII] 6087	16.72	8.13	9.94
[O I] 6300	4.58	1.53	1.96
H I 6563	250.79	52.20	31.11
[O II] 7325	26.26	6.47	3.42

[a] ines have been dereddened using E(B-V)=0.32.

[b] UV fluxes are 10^{-12} erg sec^{-1} cm^{-2}

[c] Optical fluxes are relative. Scale factors for day 300, 400 and 500 are 6 respectively.

estimate of the reddening we looked at the bolometric lightcurve. If we apply a reddening correction of 0.36 we find that there is a deviation from constant flux. If we instead lower our reddening value to 0.32 we are able to maintain a constant flux while still removing most of the interstellar absorption feature in the UV. Therefore we have chosen E(B-V)=0.32 as our reddening value for our analysis. If we apply this reddening value and the range of distances to the nova from the literature (1.5-3 kpc) to the bolometric flux (Shore et. al 1994) we find the luminosity of the nova to be 1-4$\times10^{38}$ erg s^1 cm^{-2}. This is roughly the Eddington luminosity for a 1M$_\odot$ WD.

The FOS spectrum also provided serendipitous support for our previous study of the X-ray turnoff for V1974 Cyg (Figure 2). The FOS observation occurred soon after our last GHRS low resolution spectrum (1995 Sept. 28) (Shore et al. 1997). Comparing this GHRS large aperture (2 arcsec) low resolution spectrum with the FOS data shows that the emission line fluxes have changed significantly due to recombination following the X-ray turnoff, which occurred before the GHRS spectrum was obtained. At this stage in the evolution of the ejecta ($\sim$1300 days after outburst), the helium recombination timescale was approximately one month for the densities of about 1×10^6cm^{-3}. The integrated line flux of He II 1640Å decreases by about 20% between these two observations that are roughly two months apart, from 1.26×10^{-13} (GHRS) to 1.06×10^{-13} erg s^{-1}cm^{-1} (FOS). Since both spectra were obtained with the large aperture, which completely contained the then-resolved ejecta, and the continua agree in intensity and slope, the change cannot be merely instrumental in origin. It thus appears that the bulk of the emission came from regions with densities that are characteristic of the clumps and there was little emission from the diffuse gas (see also below).

4. Analysis

We use Cloudy 94.00 (Ferland et al. 1998) to model the relative line strengths of Cyg 92 on three epochs independently. In the past we used this method to determine the physical characteristics of many other novae (Vanlandingham et al. 1996, 1997, 1999; Schwarz et al. 1997, 2001, 2002). Cloudy simultaneously solves the equations of statistical and thermal equilibrium for specified initial physical conditions; the model parameters are the spectral energy distribution of the continuum source, its temperature and luminosity, the hydrogen density, the density law for the ejecta (given by α, where $\rho \propto r^\alpha$), the inner and outer radii of the shell, the geometry of the shell, the covering and filling factors of the shell, the filling factor law (defined in the same way as the density law) and the elemental abundances (relative to solar). We adopt a blackbody to model the incident continuum. Our previous work with other novae has shown that using a model other than a blackbody for the underlying continuum source results in little difference in the model fit for this interval in the outburst (Schwarz 2002). We ran models for one of the dates using a NLTE model planetary nebula nuclei (Rauch 1997) as the continuum source instead of a blackbody and were able to achieve the same fit to the data with changing only the temperature of the source by

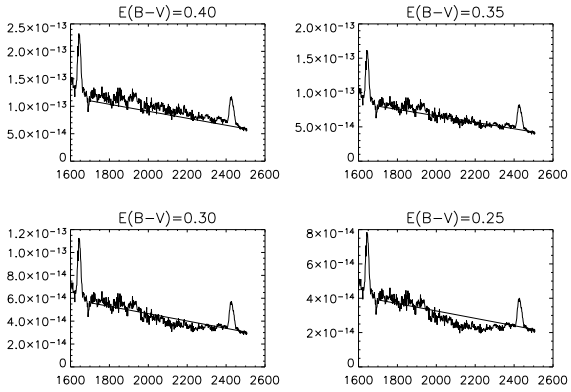

Fig. 1.— The FOS spectra are shown here dereddened using several different E(B-V) values. A rough line is fit to the continuum in each plot. These data clearly favor the higher reddening values.

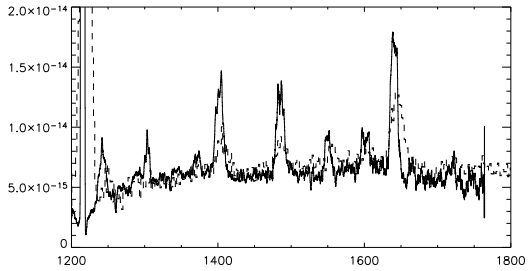

Fig. 2.— A comparision of the FOS and GHRS spectra. The GHRS spectrum (solid line) was taken on 1995 Sept. 28 and the FOS spectrum (dashed line) was taken on 1995 Nov. 30. The flux in the emission lines has decreased significantly between the two observations. No reddening correction has been applied.

less than 10%. While it has been found by Balman et. al (1998) that blackbodies cannot be used to fit the soft X-ray observations, we are not attempting to reproduce the spectral energy distribution of the incident source so blackbodies give adequate results. We can constrain the radiation temperature of the source using published X-ray observations (Balman et. al 1998), and the hydrogen density by observing the relative strengths of various ionization stages of a given element. The FWHM of the emission lines and the terminal velocities of the P Cygni profiles provide the minimum and maximum velocities of the ejecta and at any time since outburst, these are used to determine an inner and outer radius of the nova shell. Based on the luminosities derived for other ONeMg novae, we choose a starting value of 1×10^{38} erg s^{-1} and then allow the luminosity to vary with successive iterations of the code. We assume a spherical geometry for the shell, and start with a covering factor of unity. We choose an initial value for the filling factor of 0.1, since previous studies have shown that novae do not eject homogeneous shells but rather clumps of gas imbedded in a diffuse gas (Shore et al. 1993).

To determine the goodness of the fit of the model spectrum to the observed spectrum we use the χ^2 of the model:

$$\chi^2 = \sum \frac{(M_i - O_i)^2}{\sigma_i^2} \qquad (1)$$

where M_i is the modeled line flux ratio, O_i is the observed line flux ratio, and σ_i is the error in the measurement of the observed flux for each line (A96). The error is determined by measuring the line flux several times and looking at the variation

of the measurements. The variation between measurements is primarily due to the placement of the continuum and therefore the weakest lines have the largest errors. The flux for blended lines was estimated using the 'deblend' option in the IRAF 'splot' package. These lines also have higher errors than the average. These are typically on the order of 20% for the strongest lines but may be as high as 50% for the weakest or blended lines. From our observations we typically have ∼30 emission lines on which to base our fit. Of the 24 input parameters in Cloudy, we fix 13: the density power law, the filling factor and its power law, the inner and outer radii, the geometry of the shell, and 7 abundances for which we had no data. This usually left us with ∼11 free parameters and ∼19 degrees of freedom. A model is considered a good fit if it has a reduced χ^2 (defined as the χ^2 divided by the degrees of freedom) equal to one.

5. Modeling the Spectra

We modeled the same spectra described in A96 roughly corresponding to 300, 400 and 500 days after outburst. The day 300 analysis is based on the IUE spectra of 1992 December 4 combined with an optical spectrum from 1992 December 15. Day 400 is represented by the IUE spectra from 1993 April 4 and an optical spectrum from 1993 March 16. We encountered an apparent calibration error in the LWP spectrum for this date. In Figure 3 we have plotted the dereddened SWP and LWP spectra for Day 400 with a line fit to the SWP continuum. The LWP continuum appears to be too low. We can be somewhat confident that the problem is with the LWP spectrum rather than the SWP spectrum since there are two SWP spectra taken on this date and they agree with one another. If we multiply the LWP spectrum by a factor of ten then the fit is much better. While this is an eye estimate, the two spectra match reasonably well if a multiplication factor anywhere between 8 and 12 is used. This uncertainty in the calibration of the LWP spectrum results in a 20% uncertainty in the line flux ratio for the three emission lines obtained from this spectrum. Lastly, our Day 500 analysis consists of the IUE spectrum from 1993 July 2 and an optical spectrum from 1993 July 17. There appeared to be a problem with the LWP spectrum on July 2, most likely due to scattered light, so only the SWP spectrum was used for this date. The dates for the UV and optical spectra do not match exactly for each of these pairings however, due to the fact that the nova is evolving very slowly this late after the outburst, this does not present a problem.

5.1. One-Component Model

The first date we modeled was Day 300. We used 29 emission lines in our fit (see Table 2). The resulting values for the physical parameters and elemental abundances are given in Table 4. All parameters are in cgs unit. The luminosity is given in erg s^{-1}, the density in g cm^{-3}, and the radii are in cm. All abundances are given by number relative to hydrogen relative to solar. The fit has a χ^2=28 which gives a reduced χ^2 of 1.6. The number in parentheses next to the abundance in Table 4 is the number of spectral lines that were used to determine that abundance. The greater the number of lines the more constrained the value of

the abundance. Thus the abundances of magnesium and iron are much more uncertain being based solely on the fit to one spectral line, although they are probably accurate to within a factor of 5-10.

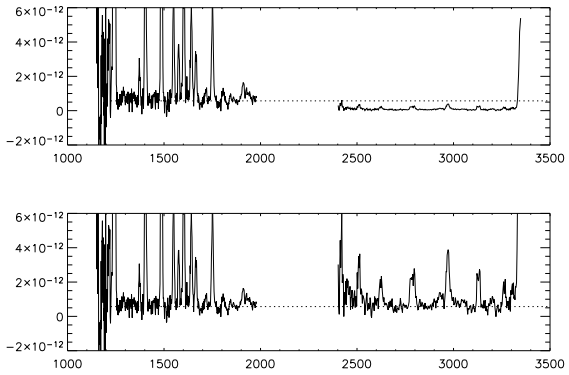

Fig. 3.— The top box shows the SWP+LWP spectra for Day 400 with a reddening correction of 0.32 applied. A rough line has been fit to the SWP continuum. The bottom box shows the same spectra but with the LWP flux multiplied by a factor of 10. The fit to the LWP continuum is much improved.

Table 2: Day 300 Observed and Model Line Flux Ratios[a]

Line ID	Observed Ratio	1-component Model Ratio	χ^2	2-component Model Ratio	χ^2
N V 1240	29.33	25.14	0.23	30.90	0.03
O IV] 1402	9.58	6.74	0.55	8.81	0.04
N IV] 1486	15.77	16.97	0.07	15.43	0.01
C IV 1549	5.64	6.00	0.05	5.78	0.01
[Ne V] 1575	2.68	2.08	0.55	2.50	0.05
[Ne IV] 1602	7.34	7.00	0.02	7.60	0.01
He II 1640	4.26	4.33	0.003	4.81	0.19
O III] 1663	4.03	6.00	2.65	5.90	2.39
N III] 1750	6.90	7.41	0.06	5.94	0.22
C III] 1909	1.92	1.99	0.01	1.70	0.16
[Ne IV] 2424	1.22	0.21	2.73	1.43	0.13
Mg II 2798	4.02	3.85	0.02	3.99	0.00
[Ne V] 2976	1.82	0.70	4.23	0.84	3.26
[Ne V] 3346	18.94	-	10	17.19	0.21
[Ne V] 3426	51.37	-	10	47.06	0.18
[Ne III] 3869	10.93	14.40	2.52	11.32	0.03
[Ne III] 3968	3.50	4.34	1.45	3.41	0.02
H I 4102	0.73	0.29	1.43	0.28	1.50
H I 4340	0.42	0.50	0.48	0.49	0.36
[O III] 4363	3.61	2.58	0.91	2.69	0.71
He II 4686	0.63	0.56	0.14	0.64	0.01
[Ne IV] 4721	2.31	1.61	1.01	1.75	0.65
H IV 4861	1.00	1.00	0.00	1.00	0.00
[O III] 4959	2.33	0.67	3.18	0.83	2.60
[O III] 5007	6.63	1.93	3.14	2.39	2.56
[N II] 5755	0.19	0.16	0.27	0.14	0.98
He I 5876	0.12	0.12	0.002	0.07	0.90
[Fe VII] 6087	0.19	0.15	0.36	0.18	0.04
[O I] 6300	0.05	0.06	0.18	0.09	3.65
H I 6563	2.93	3.26	0.13	2.99	0.00
[O II] 7325	0.31	0.20	1.24	0.24	0.58
Total χ^2			28[b]		22

[a]Ratios are relative to Hβ

[b][Ne V] 3346, 3426ÅÅ are not included in the total χ^2 of this model

Table 3: Day 400 & 500 Observed and Model Line Flux Ratios[a]

	Observed	Day 400		Observed	Day 500	
Line ID	Ratio	Model Ratio	χ^2	Ratio	Model Ratio	χ^2
N V 1240	66.64	84.80	0.83	96.37	92.58	0.02
O V 1371	1.78	1.15	0.78	-	-	-
O IV] 1402	10.86	9.99	0.04	11.36	4.29	2.42
N IV] 1486	18.71	17.52	0.05	20.87	18.24	0.18
C IV 1549	5.83	6.67	0.23	7.67	7.57	0.00
[Ne V] 1575	3.21	2.71	0.26	4.34	1.72	4.04
[Ne IV] 1602	8.90	4.19	3.11	9.16	2.80	5.36
He II 1640	5.26	6.16	0.32	7.72	8.27	0.06
O III] 1663	3.35	4.39	1.07	5.52	2.68	2.94
N IV 1719	1.29	0.35	3.34	1.39	0.33	3.63
N III] 1750	6.00	4.12	1.09	7.58	5.51	0.83
C III] 1909	1.77	0.92	2.55	1.90	1.14	1.76
[Ne IV] 2424	5.98	0.45	3.43	-	-	-
Mg II 2798	5.52	3.28	1.03	-	-	-
[Ne V] 2976	5.36	0.91	7.67	-	-	-
[Ne V] 3346	25.50	21.49	0.62	26.70	16.48	3.66
[Ne V] 3426	76.32	58.83	1.31	80.58	45.13	4.84
[Ne III] 3869	11.39	11.58	0.01	10.84	10.18	0.09
[Ne III] 3968	3.34	3.49	0.05	3.12	3.07	0.01
H I 4102	0.55	0.28	0.98	0.46	0.27	0.66
H I 4340	0.40	0.49	0.58	0.46	0.48	0.02
[O III] 4363	3.76	3.96	0.03	3.81	2.53	1.24
He II 4686	0.77	0.82	0.03	1.13	1.10	0.01
[Ne IV] 4721	2.60	0.97	4.38	2.27	0.64	5.70
H IV 4861	1.00	1.00	0.00	1.00	1.00	0.00
[O III] 4959	3.05	2.33	0.35	4.12	1.93	1.77
[O III] 5007	8.37	6.73	0.24	11.22	5.57	1.59
[N II] 5755	0.41	0.13	5.13	0.69	0.20	5.64
He I 5876	0.07	0.08	0.18	0.08	0.07	0.27
[Fe VII] 6087	0.34	0.40	0.21	0.71	0.88	0.32
[O I] 6300	0.06	0.11	3.10	0.14	0.13	0.02
H I 6563	2.17	2.94	1.40	2.23	2.88	0.93
[O II] 7325	0.27	0.23	0.21	0.25	0.20	0.39
Total χ^2			45			48

[a]Ratios are relative to Hβ

Table 4: Nova Cyg 92 Model Parameters

Parameter	One-Component Day 300	Two-Component Day 300	Two-Component Day 400	Two-Component Day 500
log(T_{BB}) K	5.52	5.52	5.67	5.65
log(L) erg s^{-1}	38.06	38.06	38.37	38.1
log(H_{den})(diffuse) g cm^{-3}	-	7.097	6.99	6.79
log(H_{den})(clump) g cm^{-3}	7.75	7.75	7.39	7.1
α	-3.0	-3.0	-3.0	-3.0
log(R_{in}) cm	15.317	15.317	15.44	15.54
log(R_{out}) cm	15.715	15.715	15.84	15.94
Fill	0.1	0.1	0.1	0.1
Power	0.0	0.0	0.0	0.0
Cover(diffuse)	-	0.5	0.62	0.47
Cover(clump)	0.3	0.32	0.33	0.18
He[a]	1.1(3)	1.0 (3)	1.3 (3)	1.4 (3)
C[a]	0.40(2)	0.69 (2)	0.87 (2)	0.59 (2)
N[a]	21.4(4)	35.5 (4)	57.6 (5)	41.7 (5)
O[a]	3.9(7)	12.3 (7)	19.5 (8)	6.5 (7)
Ne[a]	38.2(7)	56.5 (9)	44.9 (8)	23.0 (7)
Mg[a]	1.3(1)	2.6 (1)	6.5 (1)	1.0 (0)
Fe[a]	1.7(1)	1.3 (1)	3.8 (1)	9.5 (1)
χ^2	28	22	45	48
Total # of lines	29	31	33	29
# of free parameters	11	13	13	12
DOF	18	18	20	17
Reduced χ^2	1.6	1.2	2.3	2.8

[a]Elements are given by number relative to hydrogen relative to solar.

Despite the low χ^2, there are several problems with this model. First, the model is unable to adequately reproduce the high ionization lines seen in the observations and in particular the [Ne V] 3324, 3426Å lines. The χ^2 quoted for the model is with these two lines removed from the fit, each of which have an individual χ^2 of $\sim$10. This is disconcerting since these are the strongest lines in the optical spectrum and hence should have small measurement errors associated with them. There is some intrinsic error introduced by the fact that these lines are at the bluest end of the spectrum where the sensitivity of the CCD drops off. However, the magnitude of the discrepancy between the observed flux and the model flux is too large to be explained by this. There are also other groups who report the flux ratios for these lines (Moro-Martín et al. 2001) and our measurements agree with theirs. The difference between the model and observations is more likely a shortcoming of the model itself. In addition to the [Ne V] lines, our initial model is also unable to reproduce the [Ne VI] 76μ/[Ne II] 128μ line ratio reported by Hayward et al. (1996). Our model predicts a value of 0.8 for this ratio while they measured a value of $\sim$ 45. Clearly, the one-component model consistently underpredicts the high ionization lines in the spectra.

5.2. A Two-Component Model

Novae ejecta are not uniform in density but rather are clumpy, with knots of high density material embedded in a more diffuse gas (Shore et al. 1993). This is seen quite clearly in HST images of Cyg 92. As a one-dimensional model, Cloudy is not well suited to represent this type of environment. To overcome this shortcoming, we have created a two-component model, one component being the clumps and the other a diffuse gas, where the resulting line fluxes from the two components are then combined. While this model is more realistic than a simple one-component model, it is still not perfect since the two components are handled separately by Cloudy when in reality they are not separate. Ideally, we would like to be able to embed the clumpy component within the diffuse component but this is beyond the abilities of Cloudy. However, we feel that our two-component model is a reasonable approximation until a better model is found. Since our initial one-component model fit a majority of the lines, we added a second component to increase the flux of the high ionization lines. Most of the model parameters for the two components should be the same. For instance, the elemental abundances are not expected to vary between the clumps and the diffuse component. However, the physical parameters, such as the density, filling factor and covering factor, will necessarily be different for each component. Going to a two-component model increases the number of free parameters and makes the task of finding a solution more difficult. In our previous analyses of other novae, one-component models fit the available observations quite well. This analysis of Cyg 92 has been the first time a one-component model has had difficulty in fitting the observations. This is due to the wealth of data at wavelengths beyond the optical and UV that we are able to use to constrain our models of Cyg 92.

We added a diffuse component with a

density that was less than the original model (now considered the 'clump' component). We again adjusted the free parameters to obtain the best fit to the observations. The addition of the second component increased the number of free parameters by 2 since we now have a second density and a second covering factor. The other parameters (shell radii, elemental abundances, etc.) were set to the same value as the first component. The fit to the individual emission lines for our best two-component model is shown in Table 3. The parameters of the model are given in Table 4. The fit has the same temperature and luminosity for the underlying source as the initial one-component model. The elemental abundances are slightly enhanced relative to the one-component model.

The best values of the covering factors for the clump and diffuse components are found to be 0.32 and 0.5, respectively. The reduced χ^2 of the fit is 1.3 which is better than our original one-component model and we now include the [Ne V] lines in the χ^2. The two-component model also improves our fit to the IR lines ratios. We find a ratio of [Ne VI]/[Ne II]=22 which is only a factor of 2 too small instead of a factor of 50. This shows that the two-component model is significantly more realistic than the simple one-component model used previously. Woodward et al. (1995) also found that [Mg VIII] 30μ/[Al VI] 36μ $\sim$4 and our two-component model predicts a ratio of 13. The fact that this is now higher than what is observed is most likely because we have set the aluminum abundance to solar. We have found in our work with other ONeMg novae that aluminum is typically enhanced (Vanlandingham et al. 1996, 1997, 1999). We do observe lines of aluminum ([Al VI] 2601Å and Al II] 2665Å) in the Cyg 92 spectra however they are too weak to measure reliably so we have not used them in our models. If we increase the abundance of aluminum to 2.4 times solar then this ratio matches the observations.

As an additional check of our models, we can use the radio and sub-millimeter observations of Cyg 92. The observations pertinent to this analysis range from 1 to 500 GHz and were obtained within $\pm$ 50 days of the Day 300 optical and UV observations (Hjellming 1996; Ivison et al. 1993; Eyres, Davis, & Bode 1996). To compare our model to the observations, the luminosity was scaled to distances of 1.5 and 3 kpc corresponding to the range of distances reported in the literature. Figure 4 shows the comparison of the model to the observations. The larger distance (solid line) is consistent with the average of the sub-millimeter observations on days 234 and 356 but not the radio data. At 1.5 kpc the model is in better agreement with the radio observations but overestimates the sub-millimeter data. The disagreement may be due to a number of factors in the model including being optically thin or having the wrong temperature. In addition, the radio images clearly showed an ellipsoidal shell whereas our models are spherical.

After finding a fit to the Day 300 data we then proceeded to use our two-component model to fit days 400 and 500. The individual emission line fits for these days are shown in Table 3 and the model parameters are given in Table 4. These later dates are not fit as well as Day 300 as there is not as much data at other

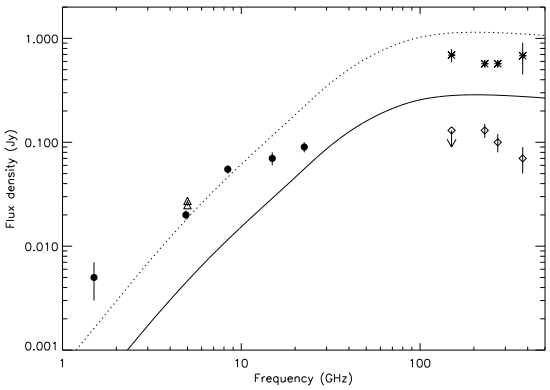

Fig. 4.— Model for Day 300 as compared to the observed radio and sub-millimeter data in the literature. The radio data are taken from Hjellming (1996) [filled circles] and Eyres et al. (1996) [day 270 and 315 = triangles]. The sub-millimeter data are from Ivison et al. (1993) [day 234 = asterisks and day 356 = diamonds]. The dotted line represents the model luminosity scaled to a distance of 1.5 kpc while the solid line is scaled to 3 kpc.

wavelengths to constrain the fits. There are some lines in Table 3 that have much large χ^2 than most of the others. Some of these, such as [Ne IV]] 1602Å and [Ne IV] 4721Å, are probably a result of the line being blended making an accurate measurement of the flux difficult. Other lines, such as N IV 1719Å and [N II] 5755Å, are weak lines which, again, increases the error in the measurement of the flux. We may have underestimated the errors for these lines in our calculation of the χ^2.

If we compare the results from all three dates, we notice some trends. The effective temperature of the continuum source increases slightly with time. This is as expected as the ejected shell expands and reveals more of the underlying WD surface. The luminosity is roughly constant, as is the covering factors of the two components. This is in agreement with the findings of Balman et al. (1998). Their X-ray observations show the effective temperature peaking at day 511 and a constant bolometric luminosity from day 255-511. The nova then turned off shortly after this at roughly day 550. The abundances values for all three dates typically agree within a factor of 2.5. All the abundances except for carbon are enhanced relative to solar values.

Based on the parameters determined from our three dates we can calculate the hydrogen ejected mass predicted by our two-component models. In order estimate the ejected mass we take the shell defined by the inner and outer radii and divide it into 1000 nested shells. The density of the innermost shell is set to the starting density of the model and is then progressed based on the density law of the model. The

filling factor is applied in the same manner. The resulting mass is then multiplied by the covering factor. Using this method, we find an ejected mass of $2.1 \pm 0.2 \times 10^{-4} M_{\odot}$, $2.8 \pm 0.3 \times 10^{-4} M_{\odot}$, and $2.1 \pm 0.2 \times 10^{-4} M_{\odot}$ for days 300, 400 and 500, respectively. The ejected mass is roughly constant over all dates, which is as expected. Shore et al. (1993) finds that the ejected mass can be calculated as $10^{-4} Y^{-1/2} M_{\odot}$, where Y is the average enhancement factor for the helium abundance. If we use this equation and an average helium abundance from our three models, we find $M_{ej} = 1.9 \times 10^{-4} M_{\odot}$, which agrees with our model values. Our masses agree fairly well with this calculation. Other groups have found ejected mass estimates for Cyg 92 (Shore et al. 1993, Krautter et al. 1996, Woodward et al. 1997) in the same range that we find here.

Table 5: Abundance Comparison

Parameter	Average from this paper [a]	A96	Moro-Martín	Hayward	Paresce
He	1.2±0.2	4.4	4.5	4.5 [b]	∼2
C	0.7±0.2	-	70.6 [b]	12 [b]	
N	44.9±11	282	50.0	50 [b]	
O	12.8±7	110	80.0	25 [b]	2-4
Ne	41.5±17	250	250.0	50	15-27
Mg	4.6±3	-	129.4 [b]	5	
Al	> 1.0[c]	-	127.5 [b]	5 [b]	
Si	-	-	146.6 [b]	6 [b]	
S	-	-	1.0	5 [b]	
Fe	4.9±4	16	8.0	4[b]	

[a] Errors given are 1σ

[b] No lines of this element are present in their spectra

[c] This is a rough estimate based on the IR line ratios

6. Comparison to other results

The first extensive analysis of the optical and UV data was done by A96 using an older version of the Cloudy code. As mentioned earlier, A96 made an error in applying the reddening corrections to their fluxes. Moro-Martín et al. (2001) and Hayward et al. (1996) also conducted abundance analyses of Cyg 92 using Cloudy. Unfortunately, both of these groups based their modeling on the results of A96 and hence propagated the errors from that analysis into their work. In addition, both of these studies report abundance values for elements which are not represented in their spectra. It is possible to predict an upper limit for a given element by increasing its abundance until the model produces emission lines that should have been seen but are not seen in the data. These two groups, however, report such large abundances of these unseen elements that emission lines would have been easily seen in the spectrum.

A third analysis is found in the literature. Paresce et al. (1995) gave rough abundances values for a few elements determined by using Cloudy on a specific "knot" of material from their HST spectra. These results, shown in Table 5, did not rely on the analysis of A96. They state that their results are lower limits on the abundances.

Finally we note that Shore et. al (1997) took the results from A96 and propagated them forward in time to Day 1300. Using GHRS data, with a much higher S/N than that of A96, they noted that the carbon abundance found by A96 was too high.

Given the error in A96 a comparison between our results and those of Hayward and Moro-Martín would be misleading. It is not surprising that our abundance results do not agree with their results. The discovery of the error in A96 was one of the primary motivations for our re-analysis of Cyg 92. Table 5 shows our results along with those of A96, Hayward and Moro-Martín. In general, our abundances are much lower than those of the three groups. Our results are higher than those found by Paresce, however, they are not in disagreement since Paresce's numbers are lower limits.

Through our previous work we have found striking similarities between many of the ONeMg novae (Shore et. al 2003, Vanlandingham et. al 1999). A complete and thorough comparison between the abundances found here and other ONeMg novae will be the subject of a future work.

7. Conclusions

We have applied a two-component photoionization code to three separate observations of Cyg 92 and have derived the physical characteristics of the ejecta on these dates. Our initial one-component model was unable to reproduce the high ionization lines seen in the spectra. By adding a second, low density, component to our models we were able to correct this problem. We find the ejecta to be enhanced, relative to solar, in He, N, O, Ne, Mg and Fe. Carbon is found to be subsolar. Our models predict an ejected mass of $\sim 2 \times 10^{-4} M_{\odot}$ which is in agreement with what has been found for other ONeMg novae.

Our results replace the earlier analysis of A96 that contained an error in the red-

dening correction. The two other analyses in the literature (Hayward et al. (1996) & Moro-Martín et al. (2001)) based their work on the results of A96 and so propagated this error into their work. Because there is such a large parameter space and many of the parameters are interdependent it is difficult to determine if a solution to one set of spectra is unique. By modeling three sets of observations independently, taken at different times during the evolution of the nova shell, we increase the confidence in our solution. If all three days arrive at the same abundance solution, then we can have much more confidence that it is the true solution. The fact that our models are able to fit the IR, radio, sub-millimeter and X-ray observations further strengthens our conclusions.

The authors would like to thank G. Ferland for use of his Cloudy photoionization code and J. Aufdenberg and J. Josè for many useful discussions. We would also like to thank the referee for a very thorough review. The referee's comments have greatly improved the quality of the paper. S. Starrfied acknowledges partial support from NSF and NASA grants to ASU; S. N. Shore acknowledges partial support from NASA grants to IUSB, and INAF 2002 and INFN/Pisa.

REFERENCES

Austin, S.J., Wagner, R.M., Starrfield, S., Shore, S.N., Sonneborn, G. & Bertram, R. 1996, AJ, 111, 869

Balman, S., Krautter, J. & Ögelman, H. 1998, ApJ, 499, 395

Chochol, D., Grygar, J., Pribulla, T., Komžik, R., Hric, L. & Elkin, V. 1997, A&A, 318, 908

Collins, P. 1992, IAUC 5454

Eyres, S. P. S., Davis, R. J. & Bode, M. F. 1996, MNRAS, 279, 249

Ferland, G.J., Korista, K.T., Verner, D.A., Ferguson, J.W., Kingdon, J.B. & Verner, E.M. 1998, PASP, 110, 761

Hayward, T.L., Saizar, P., Gehrz, R.D., Benjamin, A., Mason, C.G., Houck, J.R., Miles, J.W., Gull, G.E. & Schoenwald, J. 1996, ApJ, 469, 854

Hjellming, R. 1996, in 'Cataclysmic variables and related objects: Proceedings of the 158th colloquium of the International Astronomical Union (IAU)', 317

Ivison, R. J., Hughes, D. H., Lloyd, H. M., Bang, M. K. & Bode, M. F. 1993, MNRAS, 263, 431

Krautter, J, Ögelman, H., Starrfield, S., Wichmann, R. & Pfeffermann, E. 1996, ApJ, 456, 788

Moro-Martín, A., Garnavich, P.M. & Noriega-Crespo, A. 2001, ApJ, 121, 1636

Osterbrock, D. 1989, Astrophysics of Gaseous Nebulae and Active Galactic Nuclei (California: University Science Books)

Paresce, F., Livio, M., Hack, W. & Korista, K. 1995, A&A, 299, 823

Rauch, T. 1997, A&A, 320, 237

Schwarz, G.J. 2002, ApJ, 577, 940

Schwarz, G.J., Shore, S.N., Starrfield, S., Hauschildt, P.H., Della Valle, M., & Baron, E. 2001, MNRAS, 320, 103

Schwarz, G.J., Starrfield, S., Shore, S.N., & Hauschildt, P.H. 1997, MNRAS, 290, 75

Seaton, M.J. 1979, MNRAS, 187, 73

Shore, S.N., Sonneborn, G., Starrfield, S., Gonazlez-Riestra, R. & Ake, T.B. 1993, AJ, 106, 2408

Shore, S.N., Sonneborn, G., Starrfield, S., Gonzalez-Riestra, R. & Polidan, R.S. 1994, ApJ, 421, 344

Shore, S.N., Starrfield, S. & Sonneborn, G. 1996, ApJ, 463, L21

Shore, S.N., Starrfield, S., Ake, T.B.III & Hauschildt, P.H. 1997, ApJ, 490, 393

Shore, S.N., Schwarz, G.J., Bond, H.E., Downes, R.A., Starrfield, S., Evans, A., Gehrz, R.D., Hauschildt, P.H., Krautter, J., & Woodward, C.E. 2003, ApJ, 125, 1507

Vanlandingham, K.M., Starrfield, S., Wagner, R.M., Shore, S.N., & Sonneborn, G. 1996, MNRAS, 282, 563

Vanlandingham, K.M., Starrfield, S., & Shore, S.N. 1997, MNRAS, 290, 87

Vanlandingham, K.M., Starrfield, S., Shore, S.N., & Sonneborn, G. 1999, MMRAS, 308, 577

Woodward, C.E., Greenhouse, M.A., Gehrz, R.D., Pendleton, Y.J., Joyce, R.R., Van Buren, D., Fischer, J., Jennerjohn, N.J. & Kaminski, C.D. 1995, ApJ, 438, 921

Woodward, C.E., Gehrz, D., Jones, T.J., Lawrencem, G.F., & Skrutskie, M.F. 1997, ApJ, 477, 817

This 2-column preprint was prepared with the AAS LaTeX macros v5.2.